Sub-100 fs mode-locked erbium-doped fiber laser using a 45°-tilted fiber grating

Zuxing Zhang, Chengbo Mou,* Zhijun Yan, Kaiming Zhou, Lin Zhang, and Sergei Turitsyn

Aston Institute of Photonic Technologies, Aston University, Aston Triangle, Birmingham, B4 7ET UK
mouc1@aston.ac.uk

Abstract: We demonstrate generation of sub-100 fs pulses at 1.5 μm in a mode-locked erbium-doped fiber laser using a 45°-tilted fiber grating element. The laser features a genuine all-fiber configuration. Based on the unique polarization properties of the 45°-tilted fiber grating, we managed to produce sub-100 fs laser pulses through proper dispersion management. To the best of our knowledge, this is the shortest pulse generated from mode-locked lasers with fiber gratings. The output pulse has an average power of 8 mW, with a repetition rate of 47.8 MHz and pulse energy of 1.68 nJ. The performance of laser also matches well the theoretical simulations.

OCIS codes: (060.3735) Fiber Bragg gratings; (140.3510) Lasers, erbium; (140.4050) Mode-locked lasers.

References and links

1. H. A. Haus, K. Tamura, L. E. Nelson, and E. P. Ippen, "Stretched-Pulse Additive-Pulse Mode-Locking in Fiber ring Lasers - Theory and Experiment," IEEE J. Quantum Electron. **31**(3), 591–598 (1995).
2. K. Tamura, H. A. Haus, and E. P. Ippen, "Self-Starting Additive Pulse Mode-Locked Erbium Fiber Ring Laser," Electron. Lett. **28**(24), 2226–2228 (1992).
3. U. Keller, K. J. Weingarten, F. X. Kartner, D. Kopf, B. Braun, I. D. Jung, R. Fluck, C. Honninger, N. Matuschek, and J. Aus der Au, "Semiconductor saturable absorber mirrors (SESAM's) for femtosecond to nanosecond pulse generation in solid-state lasers," IEEE J Sel Top Quantum Electron. **2**(3), 435–453 (1996).
4. O. Okhotnikov, A. Grudinin, and M. Pessa, "Ultra-fast fibre laser systems based on SESAM technology: new horizons and applications," New J. Phys. **6**, 177 (2004).
5. S. Y. Set, H. Yaguchi, Y. Tanaka, and M. Jablonski, "Ultrafast fiber pulsed lasers incorporating carbon nanotubes," IEEE J Sel Top Quantum Electron. **10**(1), 137–146 (2004).
6. A. G. Rozhin, Y. Sakakibara, S. Namiki, M. Tokumoto, H. Kataura, and Y. Achiba, "Sub-200-fs pulsed erbium-doped fiber laser using a carbon nanotube-polyvinylalcohol mode locker," Appl. Phys. Lett. **88**(5), 051118 (2006).
7. F. Wang, A. G. Rozhin, V. Scardaci, Z. Sun, F. Hennrich, I. H. White, W. I. Milne, and A. C. Ferrari, "Wideband-tuneable, nanotube mode-locked, fibre laser," Nat. Nanotechnol. **3**(12), 738–742 (2008).
8. C. Mou, S. Sergeyev, A. Rozhin, and S. Turistyn, "All-fiber polarization locked vector soliton laser using carbon nanotubes," Opt. Lett. **36**(19), 3831–3833 (2011).
9. H. Zhang, Q. L. Bao, D. Y. Tang, L. M. Zhao, and K. Loh, "Large energy soliton erbium-doped fiber laser with a graphene-polymer composite mode locker," Appl. Phys. Lett. **95**(14), 141103 (2009).
10. T. Hasan, Z. P. Sun, F. Q. Wang, F. Bonaccorso, P. H. Tan, A. G. Rozhin, and A. C. Ferrari, "Nanotube-polymer composites for ultrafast photonics," Adv. Mater. **21**(38–39), 3874–3899 (2009).
11. Z. X. Zhang, B. Oktem, and F. O. Ilday, "All-fiber-integrated soliton-similariton laser with in-line fiber filter," Opt. Lett. **37**(17), 3489–3491 (2012).
12. Z. X. Zhang, C. Şenel, R. Hamid, and F. O. Ilday, "Sub-50 fs Yb-doped laser with anomalous-dispersion photonic crystal fiber," Opt. Lett. **38**(6), 956–958 (2013).
13. F. O. Ilday, J. R. Buckley, W. G. Clark, and F. W. Wise, "Self-similar evolution of parabolic pulses in a laser," Phys. Rev. Lett. **92**(21), 213902 (2004).
14. P. Grelu and N. Akhmediev, "Dissipative solitons for mode-locked lasers," Nat. Photonics **6**(2), 84–92 (2012).
15. B. Oktem, C. Ulgudur, and F. O. Ilday, "Soliton-similariton fibre laser," Nat. Photonics **4**(5), 307–311 (2010).
16. D. Popa, Z. Sun, T. Hasan, W. B. Cho, F. Wang, F. Torrisi, and A. C. Ferrari, "74-fs nanotube-mode-locked fiber laser," Appl. Phys. Lett. **101**(15), 153107 (2012).
17. Y. Cai, C. Zhou, M. Zhang, L. Ren, L. L. Chen, W. P. Kong, D. Q. Pang, and Z. G. Zhang, "Femtosecond Er Doped Fiber Laser Using High Modulation Depth SESAM Based on Metal/Dielectric Hybrid Mirror," Laser Phys. **19**(10), 2023–2026 (2009).
18. D. Popa, Z. Sun, F. Torrisi, T. Hasan, F. Wang, and A. C. Ferrari, "Sub 200 fs pulse generation from a graphene mode-locked fiber laser," Appl. Phys. Lett. **97**(20), 203106 (2010).

#196412 - $15.00 USD Received 26 Aug 2013; revised 23 Oct 2013; accepted 1 Nov 2013; published 11 Nov 2013

19. D. Ma, Y. Cai, C. Zhou, W. J. Zong, L. L. Chen, and Z. G. Zhang, "37.4 fs pulse generation in an Er:fiber laser at a 225 MHz repetition rate," Opt. Lett. **35**(17), 2858–2860 (2010).
20. K. M. Zhou, G. Simpson, X. F. Chen, L. Zhang, and I. Bennion, "High extinction ratio in-fiber polarizers based on 45° tilted fiber Bragg gratings," Opt. Lett. **30**(11), 1285–1287 (2005).
21. Z. J. Yan, C. B. Mou, K. M. Zhou, X. F. Chen, and L. Zhang, "UV-Inscription, Polarization-Dependant Loss Characteristics and Applications of 45 degrees Tilted Fiber Gratings," J. Lightwave Technol. **29**(18), 2715–2724 (2011).
22. S. J. Mihailov, R. B. Walker, T. J. Stocki, and D. C. Johnson, "Fabrication of tilted fibre-grating polarisation-dependent loss equaliser," Electron. Lett. **37**(5), 284–286 (2001).
23. S. J. Mihailov, R. B. Walker, P. Lu, H. Ding, X. Dai, C. Smelser, and L. Chen, "UV-induced polarisation-dependent loss (PDL) in tilted fibre Bragg gratings: application of a PDL equaliser," IEE Proc., Optoelectron. **149**(5), 211–216 (2002).
24. P. S. Westbrook, T. A. Strasser, and T. Erdogan, "In-line polarimeter using blazed fiber gratings," IEEE Photon. Technol. Lett. **12**(10), 1352–1354 (2000).
25. Z. J. Yan, C. B. Mou, H. S. Wang, K. M. Zhou, Y. S. Wang, W. Zhao, and L. Zhang, "All-fiber polarization interference filters based on 45°-tilted fiber gratings," Opt. Lett. **37**(3), 353–355 (2012).
26. C. B. Mou, K. M. Zhou, L. Zhang, and I. Bennion, "Characterization of 45 degrees-tilted fiber grating and its polarization function in fiber ring laser," J. Opt. Soc. Am. B **26**(10), 1905–1911 (2009).
27. C. B. Mou, H. Wang, B. G. Bale, K. M. Zhou, L. Zhang, and I. Bennion, "All-fiber passively mode-locked femtosecond laser using a 45º-tilted fiber grating polarization element," Opt. Express **18**(18), 18906–18911 (2010).
28. Z. J. Yan, H. S. Wang, K. M. Zhou, Y. S. Wang, C. Li, W. Zhao, and L. Zhang, "Soliton mode locking fiber laser with an all-fiber polarization interference filter," Opt. Lett. **37**(21), 4522–4524 (2012).
29. X. L. Liu, H. S. Wang, Z. J. Yan, Y. S. Wang, W. Zhao, W. Zhang, L. Zhang, Z. Yang, X. H. Hu, X. H. Li, D. Y. Shen, C. Li, and G. D. Chen, "All-fiber normal-dispersion single-polarization passively mode-locked laser based on a 45°-tilted fiber grating," Opt. Express **20**(17), 19000–19005 (2012).
30. W. H. Renninger, A. Chong, and F. W. Wise, "Pulse Shaping and Evolution in Normal-Dispersion Mode-Locked Fiber Lasers," IEEE J. Sel. Top. Quantum Electron. **18**(1), 389–398 (2012).
31. B. G. Bale, S. Boscolo, and S. K. Turitsyn, "Dissipative dispersion-managed solitons in mode-locked lasers," Opt. Lett. **34**(21), 3286–3288 (2009).
32. S. K. Turitsyn, B. G. Bale, and M. P. Fedoruk, "Dispersion-managed solitons in fibre systems and lasers," Phys. Rep. **521**(4), 135–203 (2012).

1. Introduction

Ultra-short pulse fiber lasers play an important role in the modern research and industrial applications ranging from telecom and metrology to biological/chemical applications and machining. Passive mode-locking is an efficient way of generating ultra-short femtosecond pulses. The generation of femtosecond pulses is determined by various physical effects and their complex interplay, such as group velocity dispersion (GVD) (and its compensation), self-phase modulation (SPM), gain saturation and higher-order dispersion management. Nevertheless, it is compulsory to have a mode locking mechanism in the cavity to facilitate pulse formation. To date, various mode locking elements and mechanisms have been developed including nonlinear polarization rotation (NPR) which utilizes the Kerr effect of birefringent fiber as an artificial mode locker [1,2]; semiconductor saturable absorber mirror(SESAM) [3,4] and carbon nanomaterials [5–9] which exploit nonlinear saturable optical absorption of the designated materials. The rapid development of mode-locked ultra-short pulse fiber lasers has attracted a lot of interests due to their inherent versatility, compact design, and excellent heat dissipation performance. The fiber format is also very attractive due to the intrinsic compatibility to the telecom fiber-optic systems. It is still, though, a major technical challenge to find the ultimate winning solution for a saturable absorber element. The SESAM has an excellent performance. However, it tends to have a higher manufacturing cost, because a complicated molecular beam epitaxy or chemical vapor deposition system is required. Carbon nanomaterials based mode lockers became very popular in the past ten years. However, at the moment, their polymer composites are lacking high power capacitance while the deposition procedure is not easy to be precisely controlled with a limited modulation capability [10]. Polarizers are a kind of low cost and widely applied components for NPR mode locking [11,12]. Bulk polarizers break down the integrity of all-fiber structure, while other implementations of in-fiber polarizers does not take the full advantage of the in-fiber structure showing less robustness and high insertion loss. On the other hand, the operation regimes of mode-locked fiber lasers have developed from conventional soliton to

#196412 - $15.00 USD Received 26 Aug 2013; revised 23 Oct 2013; accepted 1 Nov 2013; published 11 Nov 2013

stretched pulse, similariton [13], dissipative soliton [14], and hybrid of two different regimes [15] showing great potential of all-fiber laser systems. Various saturable absorbers have shown their capability of generating short pulse in erbium doped fiber lasers. For example, the shortest pulse generated through CNT is 74 fs [16]; SESAM can produce as short as 102 fs [17], and graphene is able to achieve a mode locked erbium fiber laser with 174 fs output duration [18]. Among these, NPR is still the most efficient way, from which 37 fs can be directly generated from a erbium doped fiber laser [19].

45°-tilted fiber grating (45TFG) is a promising type of in-fiber polarizer based on the pile-of-plate principle which taps out the *s*-light and propagates the *p*-light. Such device benefits from the all-fiber structure and low insertion loss [20,21]. The cost of such grating could also be low as they can be produced using standard UV inscription in SMF28 standard telecom fibers. Various applications have been demonstrated using 45TFG so far, such as, polarization dependent loss (PDL) equalizer [22,23], polarimeter [24] and in-fiber Lyot filter [25]. 45TFG has also been demonstrated in fiber laser applications including a single polarization CW fiber laser [26], soliton mode-locked erbium-doped fiber laser [27,28] and dissipative soliton mode-locked ytterbium doped fiber laser [29]. In this paper, we reported the shortest pulse duration generation using a 45TFG for NPR mode-locked erbium-doped fiber laser with sub-100 fs pulse duration, which operates in a dissipative stretch-pulse regime [30–32] according to our simulations.

2. Fabrication and characterization of the 45TFG

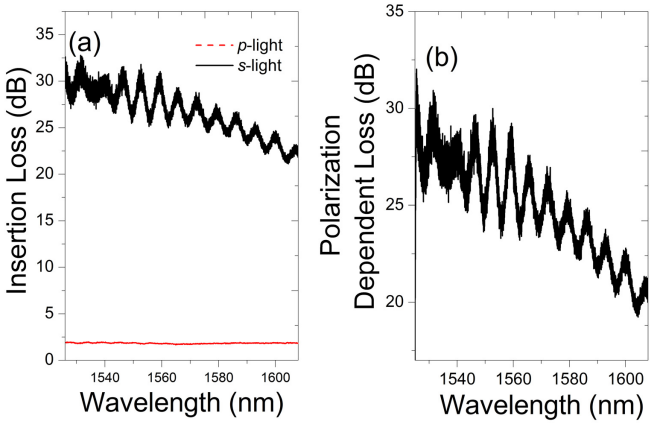

Fig. 1. Measured (a) insertion loss of *p*-light and *s*-light; (b) PDL response of the 45TFG from 1525 to 1608 nm range.

The 45°-TFGs used in the experiment were UV inscribed in a conventional telecom fiber (SMF28) using the standard phase mask scanning technique and a 244 nm UV source from a CW frequency doubled Ar^+ laser. The optical fiber samples were hydrogen loaded at 150 bar and 80°C for two days prior to the UV inscription to further enhance the fiber photosensitivity. The phase mask has a uniform period of 1800 nm (from IBSEN) and was designed to have the period pattern tilted at 33.7° with respect to the fiber axis, which would produce internal tilted index fringes at 45° in the fiber core with a broad radiation response around 1550 nm. The insertion loss and PDL of the 45°-TFG was examined by a commercial PDL test system (from LUNA system) incorporating a tunable laser which characterizes the grating in a range from 1525 nm to 1608 nm. The measured spectral range was limited by the wavelength range of the tunable laser. Fig. 1(a) shows the insertion loss of the 45TFG within the measurement range, illustrating an average ~1.7 dB insertion loss across the entire spectrum for *p*-light while a huge loss for *s*-light. As our previous work shown that *p*-light will have minimum insertion loss when the grating is tilted at exactly 45° [20,21], we

#196412 - $15.00 USD Received 26 Aug 2013; revised 23 Oct 2013; accepted 1 Nov 2013; published 11 Nov 2013

attribute this 1.7 dB insertion loss to the slight angle deviation from exact 45° tilted grating fringes. Further precise control of tilted angle may be able to optimize the insertion loss. Fig. 1(b) shows the characteristic PDL of the 45TFG over a large wavelength range (~100 nm) that covers a typical gain bandwidth of erbium doped fiber. It is clear that the PDL depends on wavelength and the maximum PDL value at 1550 nm is ~30 dB. This is in contrast to a non-tilted fiber grating in standard fiber where no noticeable PDL can be observed. One may also notice that the insertion loss and PDL have a reduction in the longer wavelength. This is mainly due to the Gaussian-like profile of the PDL response of the grating [20,21], if the central wavelength of the grating is ~1520 nm, we would expect a general reduction of PDL in the longer wavelength region. The ripples in both the insertion loss and PDL spectra were owing to the refractive index mismatch between the air and cladding [21,26]. The ripples can be removed by immersing the 45TFG in the refractive index gel while in the experiment we use a thermal shrinking polymer tube to eliminate the ripples with additional mechanical protection as well using the heat function in a standard fiber splicer.

3. Set-up and experimental results

The schematic of the 45TFG mode-locked erbium-doped fiber laser is shown in Fig. 2. The laser consists of ~1.16 m erbium-doped fiber (EDF) with nominal absorption coefficient of ~80 dB/m at 1530 nm and normal dispersion β_2 = 66.1 ps^2/km. The rest of the cavity consists of 0.43 m HI 1060 Flex fiber with anomalous dispersion of β_2 = –7 ps^2/km and 2.65 m standard telecom fiber with β_2 = –22.8 ps^2/km. Thus, the net GVD of the laser cavity is 0.013 ps^2. One polarization independent optical isolators (OIS) are used to ensure single direction oscillation. The fiber laser is pumped through a 980/1550 wavelength division multiplexing (WDM) from a grating stabilized 975 nm laser diode (LD, from 3S Photonics), which can provide up to 300 mW pump power. A commercial laser diode driver and controller (Thorlabs) are used for stabilizing the pump laser. Two in-fiber polarization controllers (PC1 & PC2) are located before and after the 45°-TFG. Two 90:10 fiber couplers are employed to tap 10% of laser power out of the cavity where one is for laser outputs after the gain fiber; the other is located before the WDM for investigating the pulse dynamics inside the laser cavity.

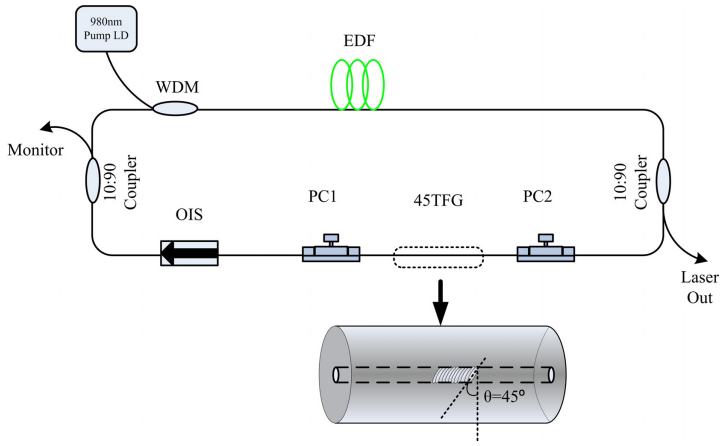

Fig. 2. Schematic of mode-locked ultrashort pulse fiber laser with 45TFG. The inset is sketch of 45TFG.

By properly adjusting the two fiber polarization controllers in the system, stable mode-locked pulses can be routinely found. The optical pulses have been directly fed through to a commercial optical autocorrelator with a nominal resolution of <1 fs without any amplification for pulse duration characterization. The lead fiber of the laser output port was cut gradually to about 2.3 m in order to optimize the obtained pulse duration. Fig. 3(a) shows the full-width half-maximum (FWHM) of autocorrelation trace is 127 fs corresponding to pulse duration of ~90 fs when Gaussian fit is assumed. Fig. 3(b) shows the optical spectrum

#196412 - $15.00 USD Received 26 Aug 2013; revised 23 Oct 2013; accepted 1 Nov 2013; published 11 Nov 2013

profile centered at 1575 nm for both output port and monitor port with a spectral bandwidth at FWHM of ~54 nm, thus giving a time-bandwidth product of ~0.58, indicating the compressed Gaussian pulse is a little beyond the transform limited. We attribute it to the third-order dispersion of the laser cavity and the outside fiber for compression. With the measured pulse duration and spectra width of the compressed pulse, the calculated pulse duration at the output point of the laser cavity is 2.4 ps. A typical pulse train is shown in Fig. 3(c) with a ~21 ns interval between two adjacent pulses, giving a repetition rate of ~47.8 MHz. We attribute the slight amplitude variation in the pulse trains to the Q-switching component in the mode locked laser because Q-switching was observed when the pump power was below the mode-locking threshold. Furthermore, fine polarization adjustment through the polarization controller may also reduce this amplitude variation. The output pulse power is 8 mW, which corresponds to the output energy of ~1.68 nJ. Fig. 3(d) shows the RF spectrum of laser at fundamental frequency showing a high signal to noise ratio of ~65 dB. The laser is stable under laboratory condition for >24 hours. Although many modern mode-locked lasers provide higher energy pulses with shorter durations, here we have realized the genuine all-fiber mode-locked ultrashort laser using the 45°-TFG. It is noted that the output spectra from the different ports have almost the same spectral profile and width, except distinct power difference. Since the net GVD is slightly normal, the laser works in a dissipative stretch-pulse regime, which will be validated in our simulations.

4. Simulations

To understand the main features of pulse evolution in this fiber laser, we performed a numerical simulation of the laser based on the modified nonlinear Schrödinger equation with the standard split-step Fourier method:

$$\frac{\partial A}{\partial z} = -\frac{i}{2}\left(\beta_2 + igT_2^2\right)\frac{\partial^2 A}{\partial T^2} + \frac{\beta_3}{6}\frac{\partial^3 A}{\partial T^3} + i\gamma|A|^2 A + \frac{1}{2}(g-a)A + i\gamma T_R \frac{\partial |A|^2}{\partial T} A \quad (1)$$

here A is the slowly varying amplitude of the pulse envelop, z and T are the propagation and time delay parameters, β_2 and β_3 are the second- and third-order dispersion, and γ is the nonlinear parameter. The gain is described by $g = g_0/(1+E/E_{sat})$, where g_0 is the small signal gain (corresponding to 30 dB in power), E is the pulse energy, and E_{sat} is the gain saturation energy. T_2 is the dipole relaxation time, T_R is related to the Raman effect, and α is the loss in the cavity. To initiate and sustain mode locking of the fiber laser, the nonlinear polarization rotation technique is used in our laser design. Here the mode-locking regime for the sake of clarity is modeled by a simple transfer function: $T_{trans} = 1 - l_0/(1+P/P_{sat})$, where l_0 is the unsaturated loss, P is the pulse power, and P_{sat} is the saturation power. We would like to point out that we do not aim here at the comprehensive comparison of numerical modeling and experiments and intentionally consider simplified description of some key effects. Instead, we would like to highlight using this simple model to study the main features of generated pulse propagation regime.

The numerical model is solved with a standard symmetric split-step beam propagation algorithm, and the initial field is white noise. The parameters used in the numerical simulations are the same as their experimental values. In the simulation, the saturation power P_{sat} is set as 835 W, E_{sat} is 1.21 nJ, and T_R is 5 fs. The evolutions of pulse duration and spectral width in the cavity are shown in Fig. 4(a). It can be seen that that the maximum pulse duration is reached after the gain fiber, both the NPE effect and the anomalous dispersion of the SMF have the contribution of temporal compensation. The corresponding maximum pulse energy in the cavity is in the end of gain fiber and then it is coupled out of the cavity after the saturable absorber. For the spectral domain, the spectral width increases in the beginning part

#196412 - $15.00 USD Received 26 Aug 2013; revised 23 Oct 2013; accepted 1 Nov 2013; published 11 Nov 2013

of the gain fiber, and shrinks in the rest part of the gain fiber due to gain filtering and saturation effects. The spectral broadening occurs in the SMF section.

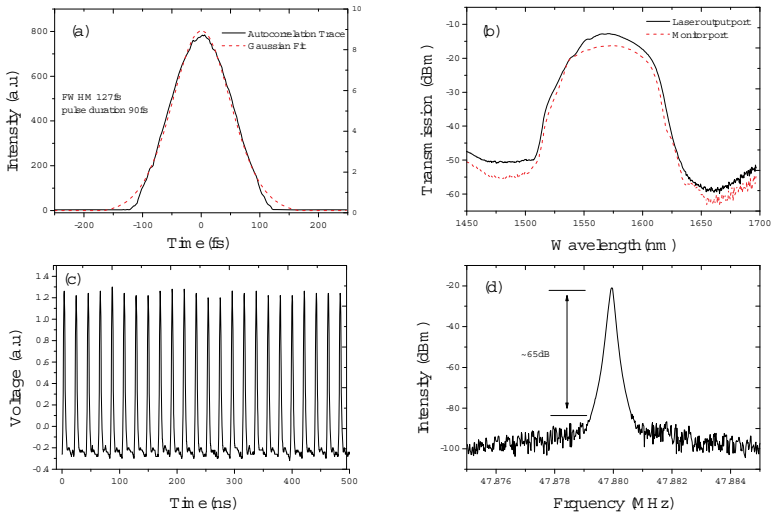

Fig. 3. Measured characteristics of laser (a) autocorrelation trace (black line) and its Gaussian fitting (red dotted line), (b) optical spectra of both output (black line) and monitor (red dotted line) ports; (c) pulse trains; (d) RF spectrum.

The simulated spectrum and pulse are shown in the Fig. 4(a) and 4(b). The simulated spectral width is 54.8 nm. And the simulated pulse duration is 2.6 ps respectively, which agrees with the estimated value according to our measured pulse duration after compression with SMF. There is a difference between the simulated and experimental spectral profiles, which we reckon is due to the simplified simulation model used. However, the whole pulse evolution within the cavity generally agrees with the experiment. According to our simulation results, the pulses in the whole cavity are always positively chirped because the net cavity GVD is normal. Meanwhile, the cavity is dispersion-managed, the pulse duration and spectral width present the typical “breath” feature. Therefore, the laser operates under the dissipative stretch-pulse regime [26–28]. The pulse duration of the current laser setup is limited by the high order dispersion, nonlinearity and total dispersion of the cavity. We believe by further decreasing the total dispersion, fiber length and proper high order dispersion management, even shorter pulse duration could be achieved.

#196412 - $15.00 USD Received 26 Aug 2013; revised 23 Oct 2013; accepted 1 Nov 2013; published 11 Nov 2013

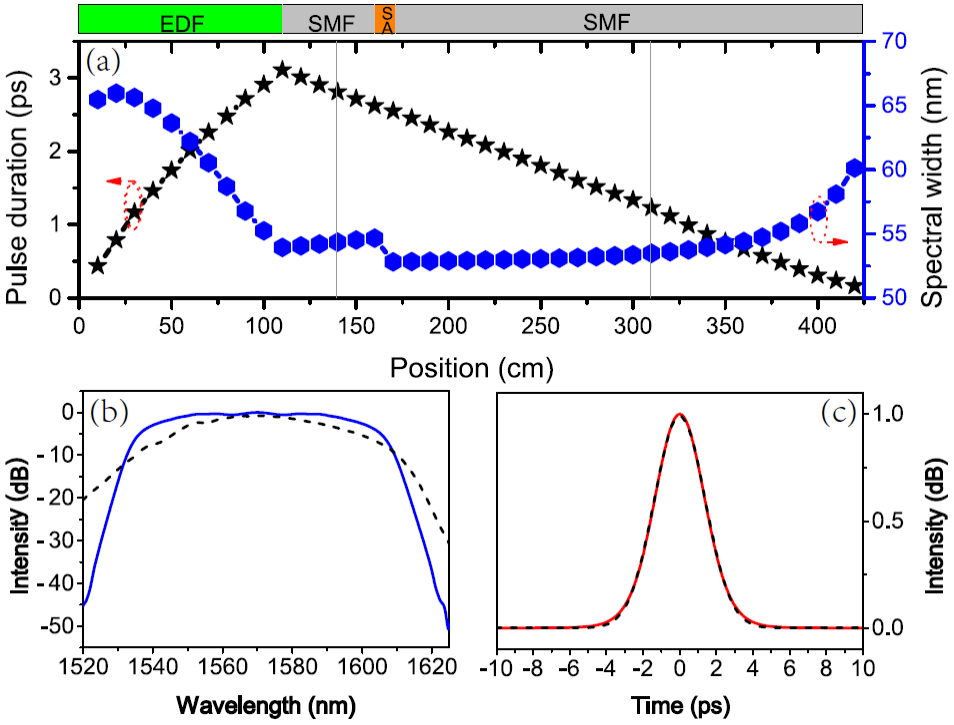

Fig. 4. (a) The simulated evolutions of pulse duration and spectral width along the cavity (the experimental output and monitor ports are indicated with grey lines), the simulated output (b) spectrum (blue real line, the black dashed line is experimental spectrum), (c) pulse (red line) and its Gaussian fitting (black dashed line).

5. Conclusions

We have demonstrated sub-100 fs pulse generation at 1.5 μm from a mode-locked erbium-doped fiber laser by using a 45°-tilted fiber grating device. The utilization of 45°-tilted fiber grating with the unique polarization property renders a compact and integrative all-fiber configuration. The dispersion management with net normal dispersion leads to the operation of dissipative stretch-pulse. To the best of our knowledge, the output pulse with pulse duration of 90 fs is the shortest pulse from fiber lasers using fiber grating for mode locking. This proves furthermore that the 45°-tilted fiber grating element is an effective and cost-efficient alternative for convention polarizers. The simulations agree rather well with the experimental results.

Acknowledgments

The authors would like to thank Dr. Youjian Song at the Ultrafast laser laboratory of Tianjin University for useful discussion. We acknowledge support of the Marie Curie IIF project DISCANT, IRSES project Telesense, and the European Regional Development Fund project: Fibre Optics and Laser Sensing Technologies Phase 2.

#196412 - $15.00 USD Received 26 Aug 2013; revised 23 Oct 2013; accepted 1 Nov 2013; published 11 Nov 2013